

Lead-Alloying Effects on the Superconducting Critical Field Curve of Indium[†]

R. C. Carriker* and C. A. Reynolds

Physics Department and Institute of Materials Science, University of Connecticut, Storrs, Connecticut

(Received 17 February 1970)

The effects of lead alloying on several features of the superconducting critical-field curve of indium have been studied. Both the anisotropy and linear effects were observed in T_c for the 0–4 at. % lead alloys. The coefficient of the linear effect K^{Pb} was measured directly and found to be $0.144^\circ\text{K}/\mu\Omega\text{ cm}$. Using the theory of Markowitz and Kadanoff, the value of the mean-squared anisotropy $\langle a^2 \rangle$ of the superconducting energy gap in indium is found to be 0.0072 ± 0.0007 , and in indium doped with lead the mean collision time for transport is found to be at least three times larger than that for the smoothing out of the gap anisotropy. The superconducting transition temperature T_c is found to increase linearly with doping in the 3–4 at. % lead concentration range. This confirms earlier work and raises a question as to why there is no unusual behavior in T_c near 3.5 at. % lead, since several other properties of the system including residual resistivity, thermoelectric power, lattice spacings, and electronic specific heat all exhibit anomalous behavior near both 3.5 and 7.0 at. % lead, whereas T_c only exhibits unusual behavior near 7.0 at. % lead. Critical-field-curve measurements in 0–0.8 at. % lead samples are found to qualitatively confirm the predictions of Clem for effects of alloying on the critical-field curve of an anisotropic superconductor. Using the analysis of Clem, $\langle a^2 \rangle = 0.007$ is found from data on $dH_c/dT|_{T_c}$. The similarity conditions on $H_0(x)/T_c(x)$ and $h(x, t)$, where x is impurity content, are found to be violated for indium doped with lead. A linear effect in $H_0(x)$ which is stronger than the linear effect in $T_c(x)$ is also observed.

INTRODUCTION

Reported herein is an investigation¹ concerned with the effects of lead alloying on the critical-field curve of indium. A great deal of theoretical work has been done in recent years analyzing the changes brought about in the critical-field curve of weak-coupling superconductors owing to doping with nonmagnetic impurities.^{2–5} Of central importance to these theories is the mean-squared anisotropy of the superconducting energy gap $\langle a^2 \rangle$. Although a value of $\langle a^2 \rangle$ for indium has previously been found² from the initial depression of the superconducting transition temperature with doping, the experimental information was limited, leading to an uncertainty in the value. The present investigation was structured so that the value of $\langle a^2 \rangle$ could be obtained in more than one way, thus allowing a confirmative check.

A second area of interest in this investigation was the variation in T_c for indium containing 3–4 at. %. Many properties of the indium-lead system have been observed to exhibit unusual behavior in the regions of 3.5 and 7.0 at. % lead. These properties include the residual resistivity,⁶ the thermoelectric power,^{7,8} the electronic specific-heat coefficient,⁹ and the lattice spacings.^{10,11} However, unusual behavior in the superconducting transition temperature has been observed only at 7.0 at. % lead and not at 3.5 at. %. Both Merriam¹² and Gyax *et al.*⁹ observed a change in dT_c/dx , where x is lead concentration, at 7.0 at. % lead, but not at 3.5 at. % lead. Because of the lack of sensitivity in these two investigations, it was felt that a very small change in dT_c/dx in the region of 3.5 at. %

might have gone undetected. In fact, careful scrutiny of the T_c -versus- x plot of Gyax *et al.* suggests that some sort of discontinuity might be present near 3.5 at. % lead. Therefore, T_c for indium containing 3–4 at. % lead was reexamined in the present investigation.

A number of investigators have studied the effects of nonmagnetic alloying on the critical temperature of weak-coupling superconductors.^{13–18} The typical behavior observed in these investigations was an initial depression in T_c with alloying, followed by a region in which T_c varied linearly with increasing solute.

Theory of Impurity Effect on T_c

Markowitz and Kadanoff² (hereafter referred to as MK) have treated the effect of nonmagnetic impurities on the critical temperature for anisotropic superconductors using a BCS-like model¹⁹ with the anisotropy introduced in the (factorable) pairing potential. MK divide the change in T_c with impurity content into two contributions: (a) an initial rapid nonlinear decrease in T_c owing to a smoothing out of the energy-gap anisotropy with doping; and (b) a linear change in T_c brought about by a gradual change in the gross properties of the system owing to increasing impurity content. They find

$$\delta T_c(\chi) = K^i \chi + \langle a^2 \rangle T_c I_c(\chi), \quad (1)$$

where χ is proportional to the impurity density (and thus the residual resistivity), $I_c(\chi)$ is a function obtained by numerical integration, and K^i is a constant dependent on the impurity and the host. The superscript i denotes that for a given host, K^i is a function of the impurity involved. The variable

χ is given by

$$\chi = \lambda^t \left(\frac{\bar{v}_F}{k_B T_c (l/\sigma)} \right) \rho_0, \quad (2)$$

where l is the electronic mean free path, σ is the absolute conductivity, \bar{v}_F is the average velocity at the Fermi surface, and ρ_0 is the residual resistivity. The factor λ^t is defined as the ratio of the relaxation time for transport (τ_{tr}) to the mean relaxation time for the smoothing out of the anisotropy of the superconducting energy gap (τ_a). The weak point in formulating δT_c as a function of ρ_0 lies in assigning a value to λ^t .

In comparing their theoretical result [Eq. (1)] with the form of the empirical relation given by Seraphim *et al.*,¹⁷ i. e., putting

$$\delta T_c(\chi) = K_1^t \chi + K_2^t \chi \ln \chi, \quad (3)$$

MK find that their result agrees well with the empirical expression for $1 < \chi < 100$. For this range of χ , MK find that their original expression for δT_c involving $I_c(\chi)$ may be replaced by the approximation

$$\delta T_c = (K^t - 0.36 \langle a^2 \rangle T_c) \chi + 0.078 \langle a^2 \rangle T_c \chi \ln \chi, \quad 1 < \chi < 100. \quad (4)$$

This equation will be used in conjunction with the expression relating χ to ρ_0 [Eq. (2)] to obtain a value of $\langle a^2 \rangle$ for indium. Also, an approximate value of λ^t for indium doped with lead will be obtained. Generally, K^t is obtained through its use as a fitting parameter for low-impurity data. In this investigation, K^t was measured directly in the linear region, which gave more confidence in the value of $\langle a^2 \rangle$ obtained.

Theory of Impurity Effect on Critical-Field-Curve Shape

Clem³⁻⁵ has extended the BCS-like model with the factorable anisotropic pairing potential of MK to study the effects of doping on the critical-field curve of a weak-coupling superconductor. As in the MK theory, effects are sought which can be related to the smoothing out of the energy-gap anisotropy.

In order to avoid linear effects,²⁰ Clem considers $h(t) (\equiv H_c/H_0)$ and a parameter \tilde{H}_0 , which he defines through

$$\tilde{H}_0^2 \equiv H_0^2 / (8\pi\gamma T_c^2), \quad (5)$$

where γ is the electronic specific-heat coefficient. Clem notes that $h(t)$ versus $t (\equiv T/T_c)$ is relatively free of linear effects and thus the reduced critical-field curve will be particularly useful in studying the anisotropy effect. Clem further notes that H_0 should exhibit linear effects similar to those exhibited by T_c . This has been verified in the case of tin by Burckbuchler *et al.*¹⁵ Clem's justification in using

the parameter \tilde{H}_0 can be seen from the BCS equations for T_c and H_0 for the isotropic case. From BCS

$$k_B T_c = 1.14 \hbar \omega \exp\{-1/[N(0)V]\} \quad (6)$$

and

$$H_0 = 1.75 [4\pi N(0)]^{1/2} k_B T_c, \quad (7)$$

where ω is a typical phonon frequency, V is the phonon-mediated attractive electron-electron interaction, and $N(0)$ is the average density of states of one spin direction at the Fermi surface. Linear effects enter both H_0 and T_c through ω , V , and $N(0)$. From these two equations, the similarity condition that H_0/T_c is a constant is seen to hold under the assumption that $N(0)$ is constant. Since $\gamma = (\frac{2}{3}) \pi^2 k_B^2 N(0)$, Clem's insertion of γ in the denominator of \tilde{H}_0^2 makes it free of all linear effects within the BCS framework.

Clem's results⁴ are formulated in terms of \tilde{H}_0 , h , t , and two additional parameters, λ and $X_H(\lambda, t)$. Clem's λ is an impurity density parameter defined as $\lambda = (2\pi T_c \tau_a)^{-1}$, thus it is essentially the χ parameter of MK (actually $\lambda = \chi/2\pi$). The factor $\chi_H(\lambda, t)$ is used to describe the effectiveness of the anisotropy corrections.

The treatment of Clem predicts a breakdown of the two commonly stated similarity conditions for the critical-field curve, namely, that $H_0(x)/T_c(x)$ and $h(x, t)$ are independent of an externally variable parameter x , where in this investigation x was impurity concentration. These predictions will be examined in the present investigation, with similarity condition on $h(x, t)$ being examined through the function

$$D(t) = h - (1 - t^2), \quad (8)$$

where $D(t)$ is known as the deviation function (deviation from parabolicity). Finally, the experimental results will be compared with the predictions of Clem for the change in slope of the critical-field curve at T_c , $dH_c/dT|_{T_c}$, as a function of the reduction in $\langle a^2 \rangle$ owing to increasing impurity content. Although a quantitative value of $\langle a^2 \rangle$ will be obtained using Clem's theory, we cannot expect a high degree of accuracy, since the maximum effects which could be expected are small, and because of experimental limitations, these maximum effects cannot be realized experimentally. Consistency in the values of $\langle a^2 \rangle$ obtained from the treatments of MK and Clem will be sought, although more confidence will be placed in the value obtained from the MK treatment of δT_c .

EXPERIMENTAL

The indium and lead used in this investigation were quoted as 99.9999% pure.²¹ Master alloys were prepared by melting together carefully weighed amounts of indium and lead under vacuum in a rock-

ing furnace. Polycrystalline samples were prepared by remelting a piece of master alloy, baking it out, pouring it into a precision bore mold,²² and then plunging it into liquid nitrogen, all steps being performed under vacuum. The specimen was then removed from the mold by etching away the glass with hydrofluoric acid, yielding a cylindrical specimen 2 mm in diam and approximately 15 cm long, 7 cm of which was selected and cut from the specimen to act as a sample. All such samples were subsequently annealed under vacuum at 110 °C for at least 160 h.

Some of the 3–4 at. % lead samples were single crystals prepared for use in another investigation as well as this one, and the crystal growing technique is described elsewhere.⁶

Determinations of the superconducting critical field H_c for various temperatures below T_c were made with the low-frequency ac field technique of Reynolds *et al.*,²³ using the cryostat, solenoids, and detection coils described by Gueths *et al.*¹⁴ and the circuitry described by Burckbuchler *et al.*¹⁵ In principle, the ac field technique involves a small alternating magnetic field (ac field) superimposed as a ripple on a much larger static magnetic field (dc field). When the dc field is just at H_c , the ac field causes super \leftrightarrow normal transitions at the ac field frequency, which by the Meissner effect can be detected by a coil wound around the sample.

Data taken for our determinations of T_c were always taken within approximately 80 m °K of T_c , or within the reduced temperature range of approximately $0.98 < t < 1.00$. It can be shown that the theoretical deviation of h from linearity for indium at $t = 0.98$ is only 0.5%. Thus, for $0.98 < t < 1.00$, one can write

$$H_c = (T_c - T) \left. \frac{dH_c}{dT} \right|_{T_c} \quad (9)$$

To obtain a T_c value, the 8–12 data points obtained near T_c were plotted on a graph of dc solenoid current versus bath pressure²⁴ at the sample. Since the temperature is a linear function of pressure²⁵ to within 0.08% for an approximate temperature range of 80 m °K near 3.4 °K, there was no necessity to calculate the temperature for each data point. A typical plot to determine T_c and $dH_c/dT|_{T_c}$ is shown in Fig. 1. Each datum point was plotted as a short vertical line corresponding to the pressure with two short horizontal bars, indicating the forward and reverse dc solenoid currents, intersecting it. Two parallel straight lines were then drawn through the forward and reverse data points so that they intersected both the horizontal and the vertical axes. For an undetermined reason, scatter was more likely to be found in the lower line, corresponding to the dc solenoid field being roughly aligned with the ambient field (mostly earth's), than with the solenoid field in the opposite

sense. This made our means of plotting the data points much more desirable than averaging the forward and reverse currents before plotting. The mean of the intersections of the two lines with the pressure axis was used to calculate T_c . The value of the slope, $dH_c/dT|_{T_c}$, was always obtained from the upper line because of the consistent absence of scatter in this line.

The accuracy of T_c determination technique was placed at ± 0.4 m °K, which was primarily limited by the uncertainty in H_c ; i. e., uncertainty in the super \leftrightarrow normal transition position. It should be noted that this accuracy is for an absolute determination and not a ΔT_c determination relative to a standard pure sample as was done by Gueths *et al.* and Burckbuchler *et al.* Their method could not be used in the present investigation owing to the wide impurity range (and thus T_c range) studied.

After T_c was determined for each sample, H_0 was determined as outlined below. This was only done for alloys from 0.04 to 0.8 at. % lead, since the ac method is not applicable to very pure samples far from T_c or to dirty alloys which become type II somewhere below T_c . The forward and reverse dc solenoid currents and temperature were determined for each datum point. Then $t (= T/T_c)$ was calculated for the data points of each sample. Obtaining a value of H_0 is necessarily a precarious procedure, since it requires extrapolating an approximately parabolic function over a large distance to absolute zero. One procedure which has been widely used is to plot h versus t^2 , relying on the approximately parabolicity of the experimentally obtained, reduced-critical-field-curve points nearest 0 °K to give a straight-line extrapolation to H_0 . This procedure is obviously lacking in accu-

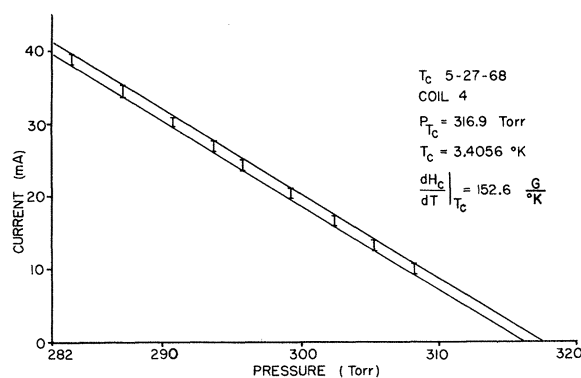


FIG. 1. Reproduction of a plot to determine T_c and $dH_c/dT|_{T_c}$. The upper line is for data taken with the dc field opposed to the ambient magnetic field and the lower line is for data taken with the dc field aligned with the ambient magnetic field.

racy, but a better technique has generally been lacking.

An improved technique based on an empirical relation put forward by Sheahen²⁶ was used to obtain H_0 values for our samples. Sheahen observes that for most soft superconductors, only three constants (H_0 , D_0 , and T_c) suffice to give the critical field when they are used in the form

$$h + D_0 \sin(\pi h) = 1 - t^2, \quad (10)$$

where D_0 is the maximum deviation from parabolicity for the particular superconductor involved. This equation cannot be used when H_0 is unknown; i. e., when we are trying to find H_0 . However, Sheahen notes that since D_0 is always small, an alternate expression which is nearly as good exists:

$$h = 1 - t^2 = D_0 \sin(\pi t^2). \quad (11)$$

Using 17 data points of Finnemore and Mapother²⁷ lying above $t^2 = 0.5$, Sheahen used H_0 and D_0 as fitting parameters to obtain a least-squares fit to Eq. (11). This procedure yielded $H_0 = 282.81$ G for indium, in excellent agreement with experimentally determined value of 282.66 G found by Finnemore and Mapother. Based on the demonstrated merit of this technique for the case of indium, we have fitted our data to Eq. (11) using a least-squares program with H_0 and D_0 as fitting parameters.

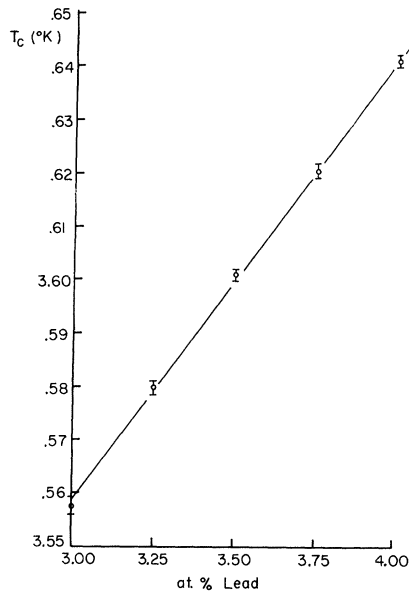


FIG. 2. Plot of T_c for indium-lead alloys as a function of lead content in the range of 3–4 at. % lead. The circles in this figure represent the average value found for 5–10 individual samples from the same master alloy. The bars are the extreme values measured for the 5–10 samples and not measurement error bars.

RESULTS AND CONCLUSIONS

T_c for Indium with 3–4 At. % Lead

Because of observed structure in the thermoelectric power, electronic specific-heat coefficient, and c/a ratio for indium doped with approximately 3.5 at. % lead, it was felt that a change in slope of the T_c -versus-at. % lead curve may have gone undetected. This was especially true in light of the observed change in slope around 7.0 at. % lead,^{9,12} which correlated well with observed structure in the other properties at this concentration. Figure 2 shows the results of this investigation on the variation in T_c with lead doping from 3.0 to 4.0 at. %. We should point out that the points in Fig. 2 represent the average value found for 5–10 individual samples from the same master alloy and that the bars are not measurement error bars, but rather the extreme values measured for the 5–10 samples. As the figure indicates, no change in slope was found in the vicinity of 3.5 at. % lead. Therefore, the results of this portion of our investigation confirm the earlier findings of Merriam and Gyax *et al.*

T_c for Indium with 0–0.8 At. % Lead

In our investigation of the variation in T_c for indium as a function of impurity (lead) concentration we were essentially interested in: (i) Presenting further verification of the theory of Markowitz and Kadanoff. (ii) Finding a more precise value of K^t for indium doped with lead (K^{Pb}) than was available. (iii) Using MK theory to obtain $\langle a^2 \rangle$ for indium and λ^t for indium doped with lead (λ^{Pb}). The experimental results are plotted in Fig. 3 as δT_c versus ρ_0 ($=\rho_{4,2}$), where ρ_0 is used as the measure of lead content. The results of Chanin, Lynton, and Serin (CLS)¹⁶ for indium doped with lead are included in Fig. 3. It can be seen from the figure that the results of both investigations are in excellent agreement over the mutually studied low-impurity range.

In finding a value for $\lambda^t \langle a^2 \rangle$, MK effectively combined Eqs. (2) and (4) to obtain

$$\delta T_c = [K^t - 0.36 \langle a^2 \rangle T_c B \lambda^t] \rho_0 + 0.078 \langle a^2 \rangle T_c B \lambda^t \rho_0 \times \ln(B \lambda^t \rho_0) \quad 1 < \lambda^t B \rho_0 < 100, \quad (12)$$

which they rearranged to have the appearance

$$\delta T_c / \rho_0 - K^t = [-0.36 + 0.078 \ln(\lambda^t B \rho_0)] \langle a^2 \rangle \lambda^t B T_c, \quad (13)$$

where

$$B = (\bar{v}_F / k_B T_c) (\sigma / l) \quad (14)$$

Here K^t has the form $(\partial T_c / \partial \rho_0)^t$ and is just the slope of the δT_c -versus- ρ_0 curve in the linear region; i. e., the slope when the gap anisotropy has been completely washed out. If it is assumed that λ^t is a constant λ for all impurities in a given

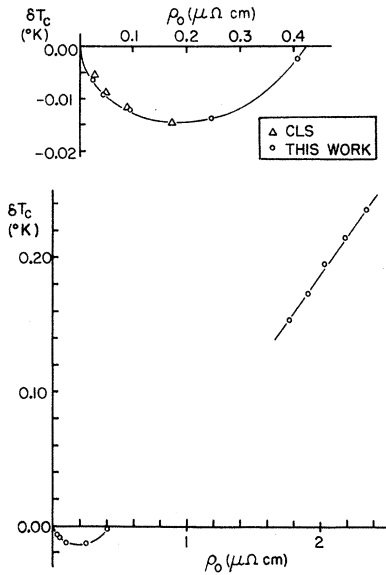


FIG. 3. Variation of T_c for indium containing 0–4 at. % lead. The points which lie on the curved line are for 0–0.8 at. % lead, and those on the straight line are for 3–4 at. % lead. The figure indicates that the agreement between the present work and CLS (Ref. 16) over the mutually studied impurity range is excellent.

host, then a plot of the left-hand side of Eq. (12) versus ρ_0 on semilog paper will give a set of parallel lines for the various impurities in the host. The relative K^i factors will be given by the vertical separation of the lines and the anisotropy effect will be given by the slope of the lines. Taking $\partial/\partial(\ln\rho_0)$ of Eq. (13), we obtain

$$\frac{\partial}{\partial(\ln\rho_0)} \left(\frac{\delta T_c}{\rho_0} - K^i \right) = 0.078 \langle a^2 \rangle \lambda^i B T_c \equiv S. \quad (15)$$

Thus if $\delta T_c/\rho_0$ [or $(\delta T_c/\rho_0) - K^i$] is plotted versus ρ_0 on semilog paper, the slope S can be measured to obtain a value of $\lambda^i \langle a^2 \rangle$. However, the problem of separating the product still remains, if we are to obtain a value for $\langle a^2 \rangle$.

What is required is one more piece of information which will allow the separation to be made. Examining the δT_c -versus- ρ_0 plot in Fig. 3, there are at least two significant features on which attention can be focused. First, there is a point at which $\delta T_c = 0$ for a finite ρ_0 ; i. e., the point at which the curve crosses the ρ_0 axis. Second, there is a point at which the slope of the curve, $d(\delta T_c)/d\rho_0$ is zero.

Setting $\delta T_c = 0$ in Eq. (12) and solving for $\langle a^2 \rangle$ yields

$$\langle a^2 \rangle = \frac{K^i}{B \lambda^i T_c [0.36 - 0.078 \ln(B \lambda^i \rho_0)]}. \quad (16)$$

Setting the derivative of Eq. (12) with respect to ρ_0 equal to zero and solving for $\langle a^2 \rangle$ yields

$$\langle a^2 \rangle = \frac{K^i}{0.075 B \lambda^i T_c [3.62 - \ln(B \lambda^i \rho_0)]}. \quad (17)$$

Now if the ρ_0 value is known for either of these two points, along with a value of K^i , a value for $\langle a^2 \rangle$ can be found as a function of λ^i . A transcendental equation in λ^i is obtained by equating $\langle a^2 \rangle$ from Eq. (15) and $\langle a^2 \rangle$ from either Eq. (16) or (17). A solution of either transcendental equation can be found by plotting the two equations from which it was obtained as $\langle a^2 \rangle$ versus λ^i and seeking an intersection of the two resulting curves, or by using a computer program which in essence does the same thing. The procedure outlined above will yield values for both $\langle a^2 \rangle$ and λ^i .

Implicit in the foregoing discussion was the assumption that the ratio of the absolute conductivity to the electronic mean free path is known for the host metal [see Eq. (14)]. Unfortunately, the values for σ/l reported in the literature by various investigators differ by a factor of as much as 3. Table I gives the values available in the literature along with the investigators and methods used. Values of $\langle a^2 \rangle$ and λ^{Pb} obtained using the different σ/l values are also given in this table. The origins of the $\langle a^2 \rangle$ and λ^{Pb} values will be discussed shortly.

We have used the procedure outlined in the last few paragraphs to obtain values of $\langle a^2 \rangle$ and λ^{Pb} . We have measured K^{Pb} directly using samples in the impurity range of 3–4 at. % lead. The plot of the data, as shown in Fig. 3, verifies that these data are in the linear region of δT_c as a function of impurity content. Based on the data from our samples, we find that $K^{\text{Pb}} = (0.144 \pm 0.001)^\circ \text{K}/\mu\Omega\text{cm}$. Values of ρ_0 for $\delta T_c = 0$ and ρ_0 for $(\partial/\partial\rho_0)(\delta T_c) = 0$ were taken from Fig. 3. It should be noted that we have slightly greater confidence in the values of $\langle a^2 \rangle$ and λ^{Pb} obtained using the value for the condition $\delta T_c = 0$. This is because there is more uncertainty in establishing the exact ρ_0 value where the curve goes through a minimum than where it crosses the ρ_0 axis. This was especially true in the present investigation, since anticipating this problem, we obtained a sample with an impurity content which would give δT_c nearly equal to zero where the curve crosses the ρ_0 axis. We find that $\rho_0 = 0.19 \pm 0.02 \mu\Omega\text{cm}$ at $(\partial/\partial\rho_0)(\delta T_c) = 0$ and $\rho_0 = 0.43 \pm 0.01 \mu\Omega\text{cm}$ at $\delta T_c = 0$ for indium doped with lead.

Our data are presented in Fig. 4(a) as $[(\delta T_c/\rho_0) - K^{\text{Pb}}]$ versus ρ_0 on a semilog plot. The dashed line was used to obtain a slope value S . We find $S = 0.198^\circ \text{K}/\mu\Omega\text{cm}$. Data points on this line fall within the requirement $1 < \chi < 100$, so that we can use the approximate formula of MK [Eq. (4)] for our analysis. It can be seen from the figure that the five points for $\rho_0 > 1.0 \mu\Omega\text{cm}$ (those for the 3–4

TABLE I Values of $\langle a^2 \rangle$ and λ^{Pb} for indium for different σ/l values available in the literature.

Method used for σ/l	Investigator	σ/l ($10^{10} \Omega^{-1} \text{cm}^{-2}$)	$\lambda^{\text{Pb}} \langle a^2 \rangle$	$\langle a^2 \rangle_1$	λ^{Pb}_1	$\langle a^2 \rangle_2$	λ^{Pb}_2
Anomalous skin effect 3×10^9 cps	Dheer (Ref. 29)	18.0 ± 1.1	0.026	0.0066	3.9	0.0079	3.3
Anomalous skin effect	CLS (Ref. 16) ^a	11.2	0.041	0.0066	6.3	0.0079	5.3
Anomalous skin effect $10^3 - 10^4$ cps	Lyall & Cochran (Ref. 30)	9.0 ± 1.6	0.051	0.0066	7.8	0.0078	6.5
Eddy-current size effect	Cotti ^b	7.88	0.058	0.0066	8.9	0.0078	7.4
dc size effect	Aleksandrov ^c	7.41	0.062	0.0066	9.5	0.0078	7.9
Theoretical	(Ref. 30)	18.9	0.024	0.0065	3.7	0.0078	3.1

^a Calculated by CLS using parameters compiled by T. E. Faber, Proc. Roy. Soc. (London) **A211**, 531 (1957).

^b P. Cotti, Physik Kondensierten Materie **3**, 40 (1964).

^c B. U. Aleksandrov, Zh. Eksperim. i Teor. Fiz. **43**, 399 (1962) [Soviet Phys. JETP **16**, 286 (1963)].

at. % lead samples) lie below the dashed line. These points lie outside the $1 < \chi < 100$ region whether or not they are included in the determination of S , and thus were not included in the determination of S . It should be pointed out that the position of these points is in good agreement with the MK theory, as can be seen by a comparison with Fig. 4(b). The solid curve in this figure is the actual MK theoretical curve and the dashed line is the empirical rule $I_c = A\chi + B\chi \ln \chi$ proposed by Seraphim *et al.*¹⁷ MK predict that data points for $\chi > 100$ should fall below the dashed line, which is just what we find. We have elected to make the comparison in this manner, since a specific value of σ/l would have to be selected to make the theoretical plot.

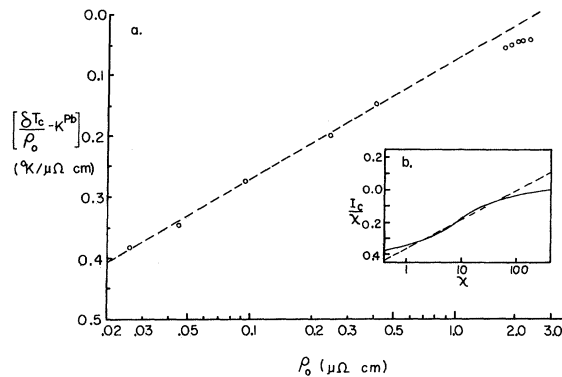


FIG. 4. (a) Plot of $[\delta T_c / \rho_0 - K^{\text{Pb}}]$ as a function of doping for indium with 0.04–4.0 at. % lead. The dashed line has a slope of $0.198 \text{ }^\circ\text{K}/\mu\Omega \text{ cm}$. The data points which lie below the line are for samples containing 3–4 at. % lead and these points are outside the range $1 < \chi < 100$. (b) MK's² theoretical plot for I_c / χ versus $\ln \chi$ (solid line) showing good agreement with empirical rule $I_c = A\chi + B\chi \ln \chi$ (dashed line) proposed by Seraphim *et al.* (Ref. 7) over the range $1 > \chi > 100$. Comparison with Fig. 4 (a) indicates that the 3–4 at. % lead data points are in the relative position predicted by MK.

Table I gives the values of $\langle a^2 \rangle$ and λ^{Pb} and their product $\lambda^{\text{Pb}} \langle a^2 \rangle$ obtained using our data and the indicated values of σ/l . Equation (15) was used to obtain the product values. Values denoted as $\langle a^2 \rangle_1$ and λ_1^{Pb} were obtained from a simultaneous solution of Eqs. (15) and (16), while those denoted as $\langle a^2 \rangle_2$ and λ_2^{Pb} were obtained from a simultaneous solution of Eqs. (15) and (17). These simultaneous solutions were obtained using machine calculations rather than plotting.

Discussion of T_c Results

MK found $\lambda \langle a^2 \rangle = 0.021$ for indium using the σ/l value given by CLS. As shown in Table I, we obtain $\lambda^{\text{Pb}} \langle a^2 \rangle = 0.041$ for In doped with Pb using the same σ/l . This difference does not present a problem, however, since MK were required to estimate S based on a limited amount of experimental data for impurities giving different S values. Perhaps the greatest uncertainty was brought about by the limited impurity ranges of the data used by MK, since for much of the data, the impurity content was insufficient to reach the minima in the δT_c behavior.

From the table it can be seen that $\langle a^2 \rangle_1$ and $\langle a^2 \rangle_2$ are in good agreement for a given σ/l , although we consider $\langle a^2 \rangle_1$ to be a better value for the reasons discussed earlier. The table also indicates that the value of $\langle a^2 \rangle$ obtained was insensitive to the value of σ/l assumed, but that the λ^{Pb} value was very sensitive to the σ/l value used. Based on all the values of $\langle a^2 \rangle$ presented in Table I, we find $\langle a^2 \rangle = 0.0072 \pm 0.007$ for indium. We have an approximate check on our value of $\langle a^2 \rangle$. MK give $\langle a^2 \rangle T_c [1/N(0)V]$ as the maximum critical-temperature depression from the anisotropy effect. By extrapolating the linear region of the δT_c -versus- ρ_0 plot to $\rho_0 = 0$ (to an intersection with the δT_c axis), the maximum δT_c the anisotropy effect itself would give in the absence of the linear effect can be found. From our data, $(\delta T_c)_{\text{max}} = 0.100 \text{ }^\circ\text{K}$. Markowitz²⁸ gives a value of $T_c [1/N(0)V] \approx 10$ for indium. Solving for

$\langle a^2 \rangle$ yields $\langle a^2 \rangle \approx 0.01$, which is in reasonable agreement with our $\langle a^2 \rangle \approx 0.007$. This check is particularly satisfying, because it does not require knowledge of λ^{Pb} .

Now we are left with determining the correct value for λ^{Pb} , which is in effect selecting the correct value of σ/l . We feel that $\sigma/l = (18.0 \pm 1.1) \times 10^{10} \Omega^{-1} \text{cm}^2$ as found by Dheer²⁹ from 3-kMc/sec anomalous-skin-effect data probably represents the best value. This work was done at the highest frequency of the ASE determinations of σ/l and the value was obtained by averaging single-crystal measurements over various orientations. The most recent determination of σ/l was made on a polycrystalline specimen of indium by Lyall and Cochran.³⁰ However, they note that the discrepancy between their value of σ/l and Dheer's (Table I) may have been due in part to a net orientation effect in their polycrystalline specimen. Based on Dheer's σ/l value, we find that $\lambda^{\text{Pb}} = 3.6 \pm 0.3$ for indium doped with lead.

This value of $\lambda^{\text{Pb}} (= \tau_{\text{tr}}/\tau_a)$ might appear to be high at first, but there is a good reason why it probably should be greater than unity. The small-angle-scattering portion of isotropic impurity scattering is relatively ineffective in contributing to the residual resistivity. However, small-angle scattering would be expected to be more effective in washing out the superconducting energy-gap anisotropy, since the direction of the maximum energy gap in \mathbf{k} space would be expected to be no more than 90° away from the direction of minimum gap. Thus τ_a would be expected to be somewhat smaller than τ_{tr} , leading to a value of λ^{Pb} greater than unity.

We note that when values of σ/l which are lower than that given by Dheer are used, the values of λ^{Pb} increase up to a maximum of 9.5. Since this high a value for λ^{Pb} seems extremely unreasonable, the present investigation might well be considered to substantiate the higher values of σ/l which have been found.

The small gap anisotropy found in the present investigation is supported by the longitudinal ultrasonic attenuation investigation of indium by Fossheim and Leibowitz.³¹ They find that in spite of a large anisotropy observed in the normal-state ultrasonic attenuation, no significant anisotropy was found in the superconducting energy gap. The small magnitude of the energy-gap anisotropy has further support in the ultrasonic attenuation measurements of Sinclair³² and Fil *et al.*³³ Although the information is insufficient to allow calculation of $\langle a^2 \rangle$, it does indicate that the maximum gap anisotropy is much smaller than that found by Morse *et al.*³⁴ in tin using the same method.

Effects on Critical-Field Curve

Now that the effects of doping on T_c for indium doped with lead have been examined, we will deal

with the effects of doping on the critical-field curve. Let us begin by examining the H_0 dependence for indium doped with lead. Once $H_0(x)$ is found (x is impurity content), we will be in a position to examine the predictions of Clem for the breakdown in the similarity conditions on $H_0(x)/T_c(x)$ and $h(x, t)$. We shall also examine change in slope of the critical-field curve at T_c , $dH_c/dT|_{T_c}$, as a function of doping that is predicted from Clem's treatment. From the analysis of Clem's predictions, we will obtain a value of $\langle a^2 \rangle$ for indium, which can be compared with that obtained from our analysis of $T_c(x)$ using MK theory.

Values of H_0 for our samples were obtained by a least-squares fit of our data for $t_2 > 0.5$ to Sheahen's empirical rule given by Eq. (11). The fitting procedure also yielded values of the maximum deviation from parabolicity, D_0 . Our least-squares-fitting procedure was checked by reproducing Sheahen's results for H_0 and D_0 using the data of Finnemore and Mapother.²⁷

Before proceeding with any discussion involving H_0 , we should point out that results involving H_0 will not have as much quantitative reliability as results on T_c and $dH_c/dT|_{T_c}$. This can be traced to several sources: (i) Considerable extrapolation is required to obtain H_0 . (ii) The uncertainty in the temperature measurements increased as the temperature was lowered. (iii) The width of the detected transitions increased with decreasing temperature.

In examining the similarity condition on H_0/T_c , it was found that the H_0 for pure indium that we would have predicted using the H_0 and δT_c values for our dilute alloys was 2.55 G below that found by Finnemore and Mapother.³⁵ Since this only represents a difference of 0.8%, it could easily be attributed to a difference in magnetic-field calibration and/or to a systematic error in our extrapolation procedure to H_0 for the alloys. Since Finnemore and Mapother's H_0 for pure indium is the generally accepted value, we have adjusted our H_0 values for the study of H_0 and H_0/T_c by adding 2.55 G to each. This allows the inclusion of Finnemore and Mapother's H_0 for pure indium in our examination of the behavior of H_0 and H_0/T_c with doping and greatly simplifies comparison with the predictions of Clem, which are in the form of fractional changes from the pure case.

The dependence of H_0 for indium on doping with up to 0.8 at. % lead is shown in Fig. 5. This figure indicates that the behavior of H_0 with increasing impurity content is qualitatively like that of T_c , with an initial depression followed by an increase with increased doping. The similarity in the behavior can be seen by comparing Fig. 5 with Fig. 3.

Similarity Condition on H_0/T_c

Let us now consider the similarity condition on

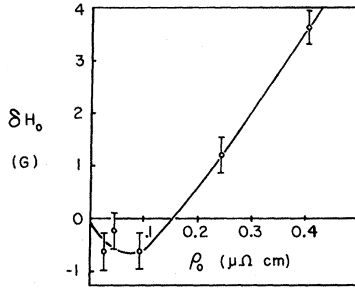


FIG. 5. Plot of the variation of H_0 for indium containing 0.04–0.8 at. % lead. The figure indicates that there is an initial depression in H_0 from the pure case followed by an increasing H_0 with doping.

H_0/T_c as given by

$$\frac{\tilde{H}_0(\lambda)}{\tilde{H}_0(0)} = \langle a^2 \rangle \delta_H(\lambda), \quad (18)$$

where

$$\tilde{H}_0(\lambda) = [\tilde{H}_0(\lambda) - \tilde{H}_0(0)], \quad (19)$$

$$\delta_H(\lambda) = X_H(0, 0) - X_H(0, \lambda), \quad (20)$$

$$\tilde{H}_0^2(\lambda) = H_0^2(\lambda) / [8\pi\gamma(\lambda)T_c^2(\lambda)]. \quad (21)$$

Equation (18) describes the expected increase in \tilde{H}_0 ($\propto H_0/T_c$) as impurities are added to a pure weak-coupling superconductor. Values of the function $\delta_H(\lambda)$ can be obtained from Fig. 3 of Clem.⁴ We recall that Clem inserted $\gamma^{1/2}$ in the denominator of \tilde{H}_0 in order to make it strictly free of linear effects within the BCS framework. To compare the predicted breakdown of the similarity condition given by Eq. (18) with the results of our experiment, it must be assumed that the change in $\gamma [= \frac{2}{3}\pi^2 k_B^2 N(0)]$ in going from 0.0 to 0.8 at. % lead can be neglected. This assumption should be reasonably valid since one would not expect $N(0)$ to change significantly over this small impurity range, and we are actually only requiring that the ratio of $[N(0)]^{1/2}$ for pure indium to that for indium doped with 0.8 at. % lead be essentially unity. In addition, good success has been obtained in the corresponding treatments of tin^{14,15} by making the same assumption.

Figure 6 demonstrates that the similarity condition on H_0/T_c is not obeyed by indium doped with lead. The solid line is the theoretical prediction of Clem based on $\langle a^2 \rangle = 0.007$ and $\lambda = 17\rho_0$ (ρ_0 in $\mu\Omega$ cm). The dashed line in the figure is the theoretical prediction based on $\langle a^2 \rangle = 0.01$. The dashed line appears to fit the data a little better than the solid one. Although the fit of the data by either theoretical curve is not particularly good, the theoretical prediction as to the qualitative behavior of H_0/T_c with doping is certainly verified. The data points in Fig. 6 suggest that a strong linear effect might

be present, and the dotted line in the figure is included simply to indicate this feature.

A few words should be said about the constant of proportionality between λ and ρ_0 . Taking the expression for χ of MK [Eq. (2)], and recalling that $\lambda = \chi/(2\pi)$, yields

$$\lambda = \frac{\lambda^i}{2\pi} \frac{\bar{v}_F}{k_B T_c (l/\sigma)} \rho_0 = \frac{1.62 \times 10^{-4}}{2\pi} \frac{\sigma}{l} \lambda^i \rho_0 \quad (22)$$

for indium, where ρ_0 is in Ω cm. Here it appears that we are again faced with selecting the proper value of σ/l . However, referring to Table I, we note that $(\sigma/l)\lambda^{Pb}$ is essentially constant, having a value of approximately $6.5 \times 10^{11} \Omega^{-1} \text{cm}^{-2}$, which when substituted into Eq. (22) yields $\lambda = 17\rho_0$.

In order to examine the similarity condition on H_0/T_c more closely, we will remove the anisotropy effect, $\delta H_{0,anis}(\lambda)$ from $\delta H_0(\lambda) = H_0(\lambda) - H_0(0)$, and examine the validity of the similarity condition for linear effects on $\delta H_0(\lambda)$. Following the procedure of Burckbuchler *et al.*,¹⁵ the change in H_0 due to the washout of the gap anisotropy is

$$\delta H_{0,anis}(\lambda) = H_0(0) \langle a^2 \rangle [I_c(\lambda) + \delta_H(\lambda)], \quad (23)$$

where $I_c(\lambda)$ is obtained from Fig. 3 of MK with $\chi = 2\pi\lambda$, and $\delta_H(\lambda)$ is obtained from Fig. 3 of Clem.⁴

The function $H_{0,anis}(\lambda)$ is independent of the impurity type. It is displayed in the lower half of Fig. 7 for $\langle a^2 \rangle = 0.007$ and $\lambda = 17\rho_0$. Data for indium doped with 0–0.8 at. % lead are shown in the upper portion of the figure. Each data point is given by $\delta H_0(\lambda) - \delta H_{0,anis}(\lambda)$; i. e., the change in $H_0(\lambda)$ due to the anisotropy effect has been subtracted out. The straight line through the data points indicates that we have successfully isolated the linear effect in δH_0 . In order to determine if the similarity condition is obeyed for linear effects, it must be determined if the linear effects on δH_0 and δT_c increase

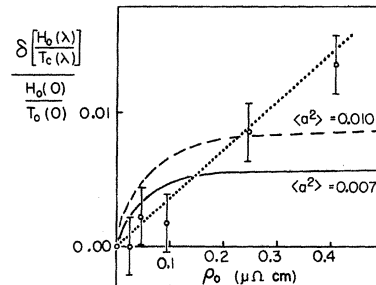


FIG. 6. Plot illustrating the breakdown of the similarity condition on $H_0(\lambda)/T_c(\lambda)$ for indium doped with lead. The solid line is the behavior predicted by Clem (Ref. 4) for a superconductor with $\langle a^2 \rangle = 0.007$ and $\lambda = 17\rho_0$. The dashed line is the behavior predicted for $\langle a^2 \rangle = 0.01$ and $\lambda = 17\rho_0$. The dotted line is merely to indicate the suspected linear effect referred to in the text.

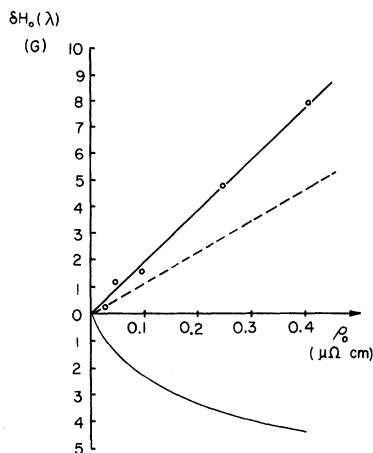


FIG. 7. The curve in the lower half of the figure is the change in H_0 due to the smoothing out of the gap anisotropy by impurity scattering which is predicted by Clem (Ref. 4) for $\langle a^2 \rangle = 0.007$ and $\lambda = 17\rho_0$. The circles were obtained by subtracting the theoretical curve from the measured change in H_0 for indium doped with lead. The dashed line represents the prediction of the similarity condition on $H_c(\lambda)/T_c(\lambda)$ after the anisotropy effect has been removed from T_c .

at the same rate with increasing impurity content. Using the linear coefficient K^{Pb} from the expression for δT_c [Eq. (12)] the similarity condition can be written as

$$\delta H_0(\lambda) - \delta H_{0,anis}(\lambda) = [H_0(0)/T_c(0)]K^{Pb}\rho_0. \quad (24)$$

The dashed line in Fig. 7 is given by this expression with $K^{Pb} = 0.144$ $^\circ\text{K}/\mu\Omega\text{cm}$. The figure indicates that the linear effect on δH_0 is not that predicted by the similarity condition, and therefore the H_0/T_c similarity condition is not obeyed by indium doped with lead. Figure 7 indicates that the linear effect is much stronger in $\delta H_0(\lambda)$ than in $\delta T_c(\lambda)$. This confirms the suspicion that a strong linear effect was present in the data displayed in Fig. 6.

The source of the stronger linear effect in $\delta H_0(\lambda)$ may possibly be due to a variation in $N(0)$ (or λ) with doping. As a first approximation we were required to ignore this variation, having no direct knowledge of it. We were encouraged by the success of Gueths *et al.*¹⁴ and Burckbuchler *et al.*¹⁵ in making this approximation for the case of tin, however, it appears that this may not be a good approximation in the case of indium doped with dilute amounts of lead (0–0.8 at. %).

Similarity Condition on $h(x, t)$

The similarity condition on $h(x, t)$ states that it is independent of the impurity concentration x , or

some other externally variable parameter. Because the differences involved in the violation of this similarity condition are very small, we have elected to examine its violation through the deviation from parabolicity [Eq. (8)]. Clem³ predicts that the deviation from parabolicity $D(t)$ will decrease, approaching the deviation for the isotropic case as the superconducting energy-gap anisotropy is washed out by impurity scattering.

The deviation from parabolicity for our samples is plotted in Fig. 8 for $0.5 \leq t^2 \leq 1.0$. The figure includes $D(t)$ for pure indium, which was obtained using the data of Finnemore and Mapother. The scale of the figure has been accentuated to show the differences between samples and the general trend indicated. This figure qualitatively supports the prediction of Clem that the washout of the gap anisotropy with increasing impurity content decreases the deviation from parabolicity.

Slope of the Critical-Field Curve at T_c

Beginning with Eq. (25) of Clem,⁴ Burckbuchler *et al.*¹⁵ have derived an expression for the change in slope with doping of the critical-field curve at T_c . They find

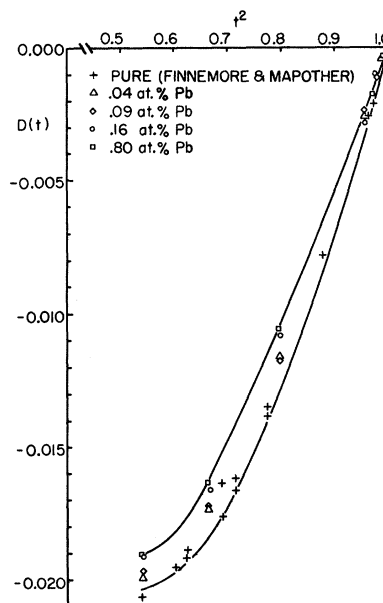


FIG. 8. The deviation from parabolicity $D(t) \equiv h - (1 - t^2)$ versus t^2 as a function of doping. The figure clearly indicates the decreasing deviation from parabolicity as lead is added to indium. The crosses are the data of Finnemore and Mapother (Ref. 27) for pure indium. The remaining data points are for this investigation. The curves are merely to emphasize the extremes; i.e., pure indium and indium doped with 0.80 at. % lead.

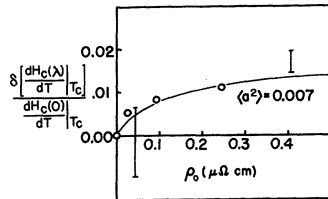


FIG. 9. The fractional change in slope of the critical-field curve at T_c as a function of doping for indium containing 0–0.80 at. % lead. The solid curve is the theoretical prediction based on Clem's treatment with $\langle a^2 \rangle = 0.007$ and $\lambda = 17\rho_0$.

$$\delta \left. \frac{dH_c(\lambda)}{dt} \right|_{T_c} / \left. \frac{dH_c(0)}{dt} \right|_{T_c} = \langle a^2 \rangle [X_H(1, 0) - X_H(1, \lambda)] + \frac{1}{2} \frac{\delta[N(0)]}{N(0)} \quad (25)$$

Again, as in the case of H_0/T_c , we will assume that the fractional variation in the density of states can be neglected.

Figure 9 shows the results of this investigation on the change in slope of the critical-field curve at T_c for dilute alloys of indium doped with lead. The solid line in the figure was obtained using Eq. (25) with $\langle a^2 \rangle = 0.007$ and $\lambda = 17\rho_0$. The figure indicates that the agreement between experiment and theory is very good in this particular case (indium doped with lead).

SUMMARY

The variation of T_c for indium with lead content (x) in the range of 3–4 at. % lead was carefully studied in the present investigation since unusual behavior is exhibited in the residual resistivity, the thermoelectric power, and the lattice spacings near 3.5 and 7.0 at. % lead, but only near 7.0 at. % lead for T_c . No change in dT_c/dx between 3.0 and 4.0 at. % lead was found. The lack of a change in dT_c/dx at 3.5 at. % lead is difficult to understand in light of the observed behavior of other properties of the system. This problem may require a careful theoretical analysis.

The superconducting transition temperature of indium doped with lead was studied for 0–4 at. % lead. Both the anisotropy effect and the linear effect were observed in these data. The coefficient

of the linear effect K^{Pb} was measured directly and found to be $0.144 \text{ }^\circ\text{K}/\mu\Omega \text{ cm}$. Using the theoretical analysis of Markowitz and Kadanoff, the product $\lambda^{Pb}\langle a^2 \rangle$ for indium doped with lead was found to be 0.041. From the information provided by our data, we were able to separate this product, yielding values of $\langle a^2 \rangle$ and λ^{Pb} . The value of $\langle a^2 \rangle$ for indium was found to be 0.0072 ± 0.0007 . The value of λ^{Pb} obtained was dependent on the value of σ/l used. Because of the wide range of σ/l values quoted in the literature for indium, the correct value of λ^{Pb} could not be precisely determined. However, the minimum and suspected best value obtained was $\lambda^{Pb} = 3.6 \pm 0.3$.

The effect of lead doping on the critical-field curve of indium was studied. The predictions of Clem for the changes brought about in the critical-field curve with doping, which have been well verified for the case of tin,^{14,15} were examined for the present case. Clem's predictions on critical-field parameters which involve $H_0(\lambda)$ were found to be qualitatively correct, and the similarity conditions on $h(\lambda, t)$ and $H_0(\lambda)/T_c(\lambda)$ were found to be violated for the case of indium doped with lead.

A linear effect in $H_0(\lambda)$ which was stronger than the linear effect in $T_c(\lambda)$ was observed. This may be due to a variation in the density of states $[N(0)]$ with doping, since in the BCS formulation, H_0 contains an extra factor of $[N(0)]^{1/2}$ which is absent in the expression for T_c . A study of the electronic specific heat γ as a function of doping (by other than superconducting critical-field methods) would be useful here, since $\gamma \propto N(0)$.

The change in slope of the critical-field curve at T_c as predicted from Clem's treatment with $\langle a^2 \rangle = 0.007$ was found to be in good agreement with the experimental findings. This value for $\langle a^2 \rangle$ is in excellent agreement with that found from the analysis of our T_c data using the theory of MK.

ACKNOWLEDGMENTS

The authors wish to thank Professor David Markowitz and Dr. F. V. Burckbuchler for their many valuable and informative discussions during the course of this investigation. In addition, we wish to thank H. Taylor for providing a ready supply of cryogenic liquids and D. Strom for a great deal of assistance in reducing the data and preparing the illustrations.

†Work supported in part by the U. S. Air Force Office of Scientific Research under Grant No. AF-AFOSR-474-67, and the Office of Naval Research, under Contract No. NONR 2967 (00).

*Present address: Hamilton Watch Co., Lancaster, Pa.

¹C. A. Reynolds and R. C. Carriker, *Bull. Am. Phys. Soc.* **14**, 129 (1969).

²D. Markowitz and L. P. Kadanoff, *Phys. Rev.* **131**, 563 (1963).

³J. R. Clem, *Ann. Phys. (N.Y.)* **40**, 268 (1966).

⁴J. R. Clem, *Phys. Rev.* **153**, 449 (1967).

⁵J. R. Clem, *Phys. Rev.* **148**, 392 (1966).

⁶R. A. Carriker and C. A. Reynolds, *Phys. Rev. B* **2**, 3140 (1970).

- ⁷W. J. Tomasch, Phys. Rev. **109**, 69 (1958).
⁸W. J. Tomasch and J. R. Reitz, Phys. Rev. **111**, 757 (1958).
⁹S. Gygax, J. S. Olsen, and R. J. Kropschot, Phys. Letters **8**, 228 (1964).
¹⁰C. Tyzack and G. Raynor, Trans. Faraday Soc. **50**, 675 (1954).
¹¹A. Moore, J. Graham, G. K. Williamson, and G. V. Raynor, Acta Met. **3**, 579 (1955).
¹²M. F. Merriam, Phys. Rev. Letters **11**, 321 (1963); Rev. Mod. Phys. **36**, 152 (1964).
¹³E. A. Lynton, B. Serin, and M. Zucker, Phys. Chem. Solids **3**, 165 (1957).
¹⁴J. E. Gueths, C. A. Reynolds, and M. A. Mitchell, Phys. Rev. **150**, 346 (1966).
¹⁵F. V. Burckbuchler, D. Markowitz, and C. A. Reynolds, Phys. Rev. **175**, 543 (1968).
¹⁶G. Chanin, E. A. Lynton, and B. Serin, Phys. Rev. **114**, 719 (1959).
¹⁷D. P. Seraphim, C. Chiou, and D. J. Quinn, Acta Met. **9**, 861 (1961).
¹⁸Y. Ohtsuka, Y. Shibuya, and T. Fukuroi, Sci. Res. Inst. Tohoku Univ. Ser. A (Japan) **15**, 67 (1963).
¹⁹J. Bardeen, L. N. Cooper, and J. R. Schrieffer, Phys. Rev. **108**, 1175 (1957).
²⁰Here "linear effects" is used in the MK context. Clem actually uses the older terminology "valence effects," which we shall avoid as being misleading.
²¹Supplied by United Mineral and Chemical Corp., New York, N. Y.
²²Precision bore Pyrex capillary with a specified i. d. of 2.000 ± 0.005 mm, supplied by the Wilmad Glass Co., Buena, N. J.
²³C. A. Reynolds, B. Serin, and L. Nesbitt, Phys. Rev. **84**, 691 (1951).
²⁴The pressure over the helium bath was measured using a Texas Instruments Model 141 servo-driven fused-quartz precision pressure gauge, and a bath height correction was made to determine the pressure at the sample position.
²⁵1958 He⁴ scale of temperatures.
²⁶T. P. Sheahen, Phys. Rev. **149**, 368 (1966).
²⁷D. K. Finnemore and D. E. Mapother, Phys. Rev. **140**, A507 (1965).
²⁸D. Markowitz, Ph.D. thesis, University of Illinois, 1963 (unpublished).
²⁹P. N. Dheer, Proc. Roy. Soc. (London) **A260**, 333 (1961).
³⁰K. R. Lyall and J. F. Cochran, Phys. Rev. **159**, 517 (1967).
³¹K. Fossheim and J. R. Leibowitz, Phys. Letters **22**, 140 (1966).
³²A. C. E. Sinclair, Proc. Phys. Soc. (London) **92**, 962 (1967).
³³V. D. Fil', O. A. Shevchenko, and P. A. Bezugly, Zh. Eksperim. i Teor. Fiz. **52**, 891 (1967) [Soviet Phys. JETP **25**, 587 (1967)].
³⁴R. W. Morse, T. Olsen, and J. D. Gavenda, Phys. Rev. Letters **3**, 15 (1959).
³⁵It should be noted that the ac field method used in this investigation was not applicable to the detection of normal \leftrightarrow super transitions for temperatures more than 80 m°K below T_c in the pure samples, since eddy currents set up by the changing flux change and caused the transition to be poorly defined.

Polaron Mass. I. The Free Polaron

John T. Marshall and Benjamin U. Stewart

Department of Physics and Astronomy, Louisiana State University, Baton Rouge, Louisiana 70803
(Received 6 July 1970)

An approximate calculation is made of the polaron effective mass as defined by Fröhlich. The approach taken is a variational one based on an extended version of Hühler's ansatz in which the trial state function employed is an exact eigenfunction of the total wave vector of the polaron. The effective mass obtained simulates the Feynman-Schultz results while the corresponding polaron self-energy is fairly accurate but inferior to the result of Feynman and Schultz.

I. DEFINITION OF PROBLEM

In a description of the motion of a single conduction electron in an ionic semiconductive crystal, Fröhlich¹ develops a Hamiltonian for a system consisting of the electron interacting with the polarization field resulting from the long-wavelength longitudinal optical modes of the crystal. The Hamiltonian is given by

$$H(\alpha) = -\frac{\partial^2}{\partial \vec{r}^2} + \sum_{\vec{v}} b_{\vec{v}}^\dagger b_{\vec{v}} + i(4\pi\alpha/S)^{1/2}$$

$$\times \sum_{\vec{v}} [(1/v)(b_{\vec{v}}^\dagger e^{-i\vec{v} \cdot \vec{r}} - b_{\vec{v}} e^{+i\vec{v} \cdot \vec{r}})], \quad (1)$$

where \vec{r} is the coordinate of the electron, $b_{\vec{v}}^\dagger$ and $b_{\vec{v}}$ are bosonic creation and destruction operators of a polarization field quantum of wave vector \vec{v} , α is a dimensionless coupling constant characteristic of the crystal, and S is the normalization volume. The limit $S \rightarrow \infty$ is to be taken with

$$\lim_{S \rightarrow \infty} \sum_{\vec{v}} = \frac{S}{8\pi^3} \int d^3v. \quad (2)$$